Robust Resource Allocation With Imperfect Channel Estimation in NOMA-Based Heterogeneous Vehicular Networks

Shengjie Guo and Xiangwei Zhou, *Senior Member, IEEE*

***Abstract*— In heterogeneous vehicular networks, *non-orthogonal multiple access* (NOMA) with effective resource allocation improves spectrum efficiency by allowing multiple users to share the same channel. However, channel estimation errors caused by high mobility in vehicular networks affect system robustness and link reliability. As a result, resource allocation in high-mobility scenarios is a challenging issue. In this paper, robust resource allocation is studied to improve both the throughput performance and reliability of NOMA-based heterogeneous vehicular networks. A cascaded Hungarian channel assignment algorithm is proposed to simplify the formulated resource allocation problem with reliability requirements into a robust power allocation problem with chance constraints. With the approximation of non-central Chi-square distribution, the chance constraints are transformed into deterministic constraints. Furthermore, the optimal power allocation for the transformed problem is obtained in consideration of the requirements in NOMA. Simulation results illustrate the effectiveness of the proposed robust resource allocation scheme and its improvement over existing schemes.**

***Index Terms*— Imperfect channel estimation, NOMA, resource allocation, vehicular communications.**

I. Introduction

WITH the explosion of information and computer technology, the *fifth generation* (5G) of wireless communications introduces new technologies and applications, such as small cell networks, reliable vehicular networks, and millimeter wave communications, which comprises an unprecedented ultra-dense and heterogeneous network environment [2], [3]. Vehicular networks play a pivotal role in 5G wireless systems and ensure the reliability and safety of vehicles. Therefore, many standardization parties and organizations have put great efforts in standards and projects of vehicular communications, such as IEEE 802.11p, the *third generation partnership project* (3GPP) *long term evolution vehicle* (LTE-V), and the *European Union Mobile and wireless communications Enablers for Twenty-twenty Information Society* (METIS) project [4].

The IEEE 802.11p, as a part of the *wireless access in vehicular environment* (WAVE) protocol, has been applied to a large number of experiments in lab and on road since its release date back to 2010 [5]. The maturity of IEEE 802.11p has been shown via its robust performance in dedicated short distance *vehicle-to-vehicle* (V2V) communications and its ability to allow fully distributed access to the channels [6]. However, the designs in physical and medium access control layers of IEEE 802.11p face several challenges, including coverage extension, reliability guarantee, and network scalability [7]–[9]. To overcome the drawbacks of IEEE 802.11p and extend the utilization of LTE networks, LTE-V was first published in 3GPP Release 14 in 2016 [10]. Two radio interfaces, the cellular and PC5 interfaces, are specified to support *vehicle-to-infrastructure* (V2I) and V2V links, respectively. As a result, the vehicular information exchange residing in cellular networks becomes a promising solution to extending coverage and ensuring reliability and scalability of vehicular networks.

Since the LTE-V is a promising alternative for vehicular communications, many recent studies have been devoted to vehicular communications in cellular networks. One of the most active areas is resource allocation. In [11], a cross-layer power allocation design has been proposed to maximize the overall throughput in a vehicular network. Through a multi-level water-filling algorithm for power allocation and a pricing strategy for relaying vehicle selection, the proposed cross-layer design has shown performance superiority to classic pricing strategies. In addition to dedicated power allocation, a joint power and channel allocation strategy for *vehicle-to-everything* (V2X) communications has been proposed in [12] based on the matching approach. Given different types of users, the hyper-graph theory has been exploited and a local search based approximation algorithm has been designed for user throughput maximization. In consideration of latency and reliability, a resource allocation solution focusing on both power control and modulation scheme has been provided in [13] for LTE V2V communication systems. Through the random network analysis and Lagrange dual decomposition, the proposed algorithm can find the optimal solution to the formulated problem.

Manuscript received May 7, 2018; revised September 10, 2018 and October 28, 2018; accepted December 2, 2018. Date of publication December 10, 2018; date of current version March 15, 2019. This work was supported in part by the National Science Foundation under Grant No. 1560437. This paper was presented at the IEEE International Symposium on Personal, Indoor and Mobile Radio Communications, Montreal, QC, October 2017 [1]. The associate editor coordinating the review of this paper and approving it for publication was H. Zhang. *(Corresponding author: Xiangwei Zhou.)*

The authors are with the Division of Electrical and Computer Engineering, Louisiana State University, Baton Rouge, LA 70803 USA (e-mail: sguo12@lsu.edu; xwzhou@lsu.edu).

Color versions of one or more of the figures in this paper are available online at http://ieeexplore.ieee.org.

Digital Object Identifier 10.1109/TCOMM.2018.2885999

However, involving massive vehicular communication links into ultra-dense and heterogeneous 5G cellular networks is a challenge. As the spectrum resource becomes more scarce in prevailing *orthogonal multiple access* (OMA) networks, *non-orthogonal multiple access* (NOMA) in vehicular networks has been studied recently to improve spectrum efficiency [14], [15]. Allowing multiple users to share the same channel, NOMA alleviates the spectrum scarcity problem. However, the interference introduced by spectrum sharing in NOMA has to be effectively handled. Furthermore, current vehicles are not only serving as transportation tools but also evolving to infotainment platforms [3]. Therefore, both reliable transmission of safety information and high-speed data transmission are required for future vehicular networks. To satisfy various requirements for V2V and V2I communications, resource allocation in vehicular communications has been extensively studied. To retain the reliability of real-time V2I transmissions, delay-aware *quality of service* (QoS) has been considered in [16]. A joint power and sub-carrier allocation scheme has been proposed to improve the energy efficiency of V2I communication networks. In [17], a resource allocation algorithm has been proposed to realize the coexistence of cognitive V2V and IEEE 802.22 networks.

Obviously, the high-mobility nature of vehicular networks renders more channel estimation errors for *vehicle users* (VUs). With more channel uncertainties in the fast changing vehicular communication environment, it is necessary to consider the imperfect *channel state information* (CSI) in resource allocation, especially for the reliability of vehicular communications. In [18], a three-state heuristic resource allocation algorithm has been proposed for device-to-device enabled V2X communications with slowly varying CSI. In [9], resource allocation based on slow fading parameters and fast fading statistical information has been studied. The ergodic capacities of V2I links and reliability requirements of V2V links have been jointly taken into consideration. A model of the channel estimation errors caused by delayed CSI feedback rather than the statistical information of the channel has been adopted in [19].

The aforementioned literature has endeavored to alleviate the spectrum scarcity problem in vehicular networks by applying NOMA with effective resource allocation in consideration of the high-mobility nature of prevailing vehicular networks. However, how to effectively allocate resource in NOMA-based vehicular networks while addressing channel uncertainties and estimation errors remains a difficult problem. Recently, resource allocation in NOMA systems with imperfect CSI has been studied [20]–[22]. In [20], user scheduling and power allocation are jointly optimized for energy-efficient NOMA systems. In consideration of imperfect CSI, a chance-constrained problem has been formulated and then transformed into a deterministic one. To reduce the computational complexity and achieve satisfactory system energy efficiency, a heuristic suboptimal user scheduling algorithm and iterative power allocation have been presented. To extend to the scenario of heterogeneous networks, the cross-tier interference has been considered in the energy-efficient resource allocation [21]. To address the energy efficiency optimization problem in multi-carrier NOMA systems, optimal resource allocation for power minimization has been explored in [22]. Both optimal and suboptimal schemes have been derived to balance the performance and computational complexity with imperfect CSI. However, the aforementioned studies mostly focus on energy efficiency and do not take channel assignment into account. Moreover, the cross-tier interference and different QoS requirements are seldom considered.

Motivated by the above, we study robust resource allocation in 5G heterogeneous vehicular networks in this paper to satisfy the QoS requirements of V2V and V2I communications. The performance of NOMA based heterogeneous vehicular networks is affected by not only imperfect CSI but also cross-tier interference. Additionally, various QoS requirements of different links need to be considered. To efficiently utilize the wireless resources, we take both channel assignment and power allocation into account in our model. In consideration of the high mobility in vehicular networks, we formulate a chance-constrained optimization problem to satisfy the strict reliability requirements in vehicular communications and at the same time to limit the cross-tier interference from *femto users* (FUs) in heterogeneous networks. Moreover, we consider NOMA in our formulation to improve spectrum efficiency. Through our analysis and design, we propose a robust resource allocation algorithm. Moreover, simulation results demonstrate the desired throughput performance and reliability. The main contributions of our paper are listed as follows.

- We model a NOMA-based heterogeneous vehicular network and formulate the corresponding chance-constrained throughput optimization problem, targeting to address the resource allocation issue in high-mobility environments with different user QoS requirements and imperfect CSI.
- Since the optimal solution requires exhaustive search with prohibited computational complexity, we propose a suboptimal method to decompose the original problem and balance the performance and computational complexity.
- To simplify the formulated problem, we propose a cascaded Hungarian channel assignment algorithm to form VU-FU pairs and assign channels. Based on different criteria, we discuss the corresponding cascaded Hungarian channel assignment schemes.
- Within each VU-FU pair, we adopt stochastic optimization and non-Chi square approximation to transform the chance constraints. Through mathematical manipulation and analysis, we find the optimal power allocation for the transformed problem.
- By building the simulation of a high-mobility heterogeneous vehicular network with a spatial Poisson point process, we illustrate that our proposed robust resource allocation scheme satisfies the various QoS requirements and effectively improves the overall throughput of V2I links, in comparison with the prevailing schemes including OMA resource allocation.

The rest of the paper is organized as follows. In Section II, the system model and our problem formulation are presented. In Section III, a cascaded Hungarian channel assignment algorithm is proposed. In Section IV, the feasible region of user powers and optimal power allocation are derived.

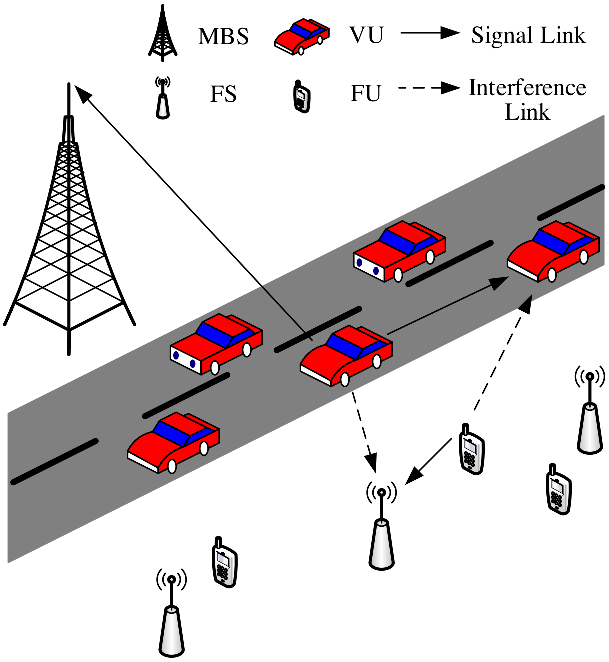

Fig. 1. System model.

In Section V, simulation results are given. Finally, conclusions are drawn in Section VI.

II. System Model and Problem Formulation

A. System Model

To satisfy various requirements of both safety-critical applications and efficient transmissions in V2X communications [14], a heterogeneous vehicular network is considered and depicted in Fig. 1, which is similar to [23] and [24] but with imperfect channel state information in the uplink. A *macro base station* (MBS) is used to provide high-speed data stream service for N VUs. *Femto stations* (FSs) coexist with the MBS and serve M FUs to offload data traffic from the MBS. There are L available channels that are enough for the orthogonal transmission of the VUs or FUs, i.e., $\max\{N, M\} \le L$. Each VU adopts NOMA to simultaneously communicate with the MBS for high-speed data service and the corresponding vehicle receivers for safety message exchange. Note that more than two links sharing the same channel is not preferable in NOMA due to the hardware complexity and processing delay [25], [26]. Therefore, we assume that each VU transmitter only has one V2V link to its closest VU receiver for safety information transmission. In the dynamic vehicular network environment, all links are set up dynamically to guarantee that the closest vehicles can communicate with each other in every time slot, which is made possible by in-vehicle sensors and the Global Positioning System. For the other VUs, the information, such as locations, speeds, and actions, when vehicle locations change can be obtained from V2I links to assist in path planning and speed control. Note that advanced dynamic user scheduling and pairing schemes may help to achieve even better performance, which will be studied in our future work. In this case, only one V2V link coexists with the V2I link of each VU transmitter over one channel through NOMA. Furthermore, each channel is reused by one FU to improve spectrum efficiency in the heterogeneous network. Therefore, one VU and one FU share the same channel and form a VU-FU coexisting pair. The entire heterogeneous network may consist of multiple coexisting pairs and different pairs use OMA to avoid interference.

In this paper, the channel model includes small-scale fast fading, shadowing, and large-scale pathloss. As in [19], we assume that the CSI of V2I links can be obtained without estimation error. This is because that V2I links are usually in line of sight and depend on the relative locations that vary slowly across different time slots due to the long distance between the MBS and VU transmitters. In such a case, the channel power gain between the i-th VU transmitter and MBS over the j-th channel, $g^v_{i,j}$, is

$$g^v_{i,j} = |h^v_{i,j}|^2 \xi_i C d_i^{-\beta} \triangleq |h^v_{i,j}|^2 \alpha_i, \tag{1}$$

where $|\cdot|$ is the norm operator, $h^v_{i,j}$ is the fast fading component of the link between the i-th VU transmitter and MBS over the j-th channel, which follows complex Gaussian distribution with zero mean and unit variance, i.e, $h^v_{i,j} \sim \mathcal{CN}(0,1)$, ξ_i is the log-normal shadowing random variable with standard deviation ζ for the link between the i-th VU transmitter and MBS, C is the pathloss constant, d_i is the distance between the i-th VU transmitter and MBS, and β is the pathloss exponent. Since each VU transmitter and its corresponding receiver have similar speeds and no obstacles in between, we can regard the V2V link channel estimation error-free. Additionally, the FUs are assumed with low mobility, and thus the *FU to FS* (F2FS) link can also be estimated precisely. The F2FS link CSIs are broadcast to the VUs.

However, due to the fast changing environment between the FUs, FSs, and VUs, the fast fading components of cross-tier interference links suffer from channel estimation errors. The estimation of interference link CSIs is pilot-based. Denote $h^v_{i,m,j}$ and $h^f_{m,i',j}$ as the fast fading components of the interference links from the i-th VU transmitter to the m-th FU's corresponding FS over the j-th channel and from the m-th FU to the i-th corresponding VU receiver, indexed by i', over the j-th channel, respectively. We have

$$h^v_{i,m,j} = \hat{h}^v_{i,m,j} + \epsilon \tag{2}$$

and

$$h^f_{m,i',j} = \hat{h}^f_{m,i',j} + \epsilon, \tag{3}$$

where $\hat{h}^v_{i,m,j} \sim \mathcal{CN}(0,1)$ and $\hat{h}^f_{m,i',j} \sim \mathcal{CN}(0,1)$ are the estimated fast fading components of the link from the i-th VU transmitter to the m-th FU's corresponding FS over the j-th channel and that from the m-th FU to the i-th corresponding VU receiver over the j-th channel, respectively, and ϵ is the channel estimation error, i.e., $\epsilon \sim \mathcal{CN}(0, \sigma^2_\epsilon)$ [27]. Given the limited transmit powers of FUs, we assume that the interference from the FUs to the MBS is negligible.

The channel power gains between the i-th VU transmitter and its corresponding receiver over the j-th channel, $g^v_{i,i',j}$, and between the m-th FU and its corresponding FS over the j-th channel, $g^f_{m,j}$, and the interference link channel power gains from the i-th VU transmitter to the m-th FU's corresponding FS over the j-th channel, $g^v_{i,m,j}$, and from the m-th FU to the i-th corresponding VU receiver over the j-th channel, $g^f_{m,i',j}$, can be similarly defined as in (1).

B. Problem Formulation

In NOMA, the MBS and VU receivers share the same channel with different link qualities. In the vehicular network scenario, the VU receiver is regarded as the near user and the MBS as the far user. The path loss usually has greater effect on and dominates the channel power gain in real V2X scenarios given the value of the path loss exponent (usually 3 to 4 in the city). Furthermore, V2V links are usually in line of sight and suffer less shadowing effect. Therefore, we assume that the power gain of V2V link, $g^v_{i,i'j}$, is larger than that of V2I link, $g^v_{i,j}$, and then the transmitted messages from the i-th VU transmitter to the MBS can be decoded and subtracted at the i-th corresponding VU receiver via *successive interference cancellation* (SIC), which is critical for NOMA systems. To successfully execute SIC at the VU receiver and correctly decode the safety information, a power difference condition needs to be satisfied [28], i.e.,

$$\frac{\sum_{j=1}^{L} a_{i,j}(P^v_i - P^v_{i,i'})g^v_{i,i',j}}{\sigma^2} \geq \delta, \tag{4}$$

where $a_{i,j}$ is the channel assignment indicator such that $a_{i,j} = 1$ when the i-th VU transmitter and its corresponding receiver occupy the j-th channel and $a_{i,j} = 0$ otherwise, P^v_i and $P^v_{i,i'}$ are the transmit powers of the i-th VU transmitter for the V2I and V2V links, respectively, σ^2 is the noise power, and δ is the minimum power difference ratio, which is related to the hardware.

With (4) satisfied, the *signal to interference noise ratio* (SINR) of the received signal at the MBS from the i-th VU transmitter can be expressed as

$$\gamma^v_i = \frac{\sum_{j=1}^{L} a_{i,j} P^v_i g^v_{i,j}}{\sum_{j=1}^{L} a_{i,j} P^v_{i,i'} g^v_{i,j} + \sigma^2}. \tag{5}$$

Due to the limited transmit powers of FUs, the interference from FUs to the MBS is neglected.

Similarly, the SINR of the received signal at the i-th VU receiver from the i-th VU transmitter is

$$\gamma^v_{i,i'} = \frac{\sum_{j=1}^{L} a_{i,j} P^v_{i,i'} g^v_{i,i',j}}{\sum_{m=1}^{M} b_{m,j} P^f_m g^f_{m,i',j} + \sigma^2} \tag{6}$$

and the SINR of the received signal at the FS from the m-th FU is

$$\gamma^f_m = \frac{\sum_{m=1}^{M} b_{m,j} P^f_m g^f_{m,j}}{\sum_{j=1}^{L} a_{i,j}(P^v_i + P^v_{i,i'}) g^v_{i,m,j} + \sigma^2}. \tag{7}$$

To satisfy various QoS requirements for different types of links, we maximize the overall throughput of V2I links while guaranteeing the reliability of V2V and F2FS links. The power allocation problem is formulated as

$$\max_{\substack{a_{i,j}, b_{m,j}, \\ P^v_i, P^v_{i,i'}, P^f_m}} \sum_{i=1}^{N} \log_2(1 + \gamma^v_i) \tag{8}$$

$$\text{s.t.: } 0 \leq P^v_i, \quad 0 \leq P^v_{i,i'}, \; 0 \leq P^v_i + P^v_{i,i'} \leq P^v_{max}, \; \forall i, \tag{8a}$$

$$\frac{\sum_{j=1}^{L} a_{i,j}(P^v_i - P^v_{i,i'})g^v_{i,i',j}}{\sigma^2} \geq \delta, \quad \forall i, \tag{8b}$$

$$0 \leq P^f_m \leq P^f_{max}, \quad \forall m, \tag{8c}$$

$$\Pr(\gamma^v_{i,i'} \geq \gamma^v_{th}) \geq 1 - p_v, \quad \forall i, \tag{8d}$$

$$\Pr(\gamma^f_m \geq \gamma^f_{th}) \geq 1 - p_f, \quad \forall m, \tag{8e}$$

$$a_{i,j}, b_{m,j} \in \{0, 1\}, \quad \forall i, j, m, \tag{8f}$$

$$\sum_{i=1}^{N} a_{i,j} \leq 1, \quad \forall j, \; \sum_{j=1}^{L} a_{i,j} \leq 1, \; \forall i, \tag{8g}$$

$$\sum_{m=1}^{M} b_{m,j} \leq 1, \quad \forall j, \; \sum_{j=1}^{L} b_{m,j} \leq 1, \; \forall m, \tag{8h}$$

where P^v_{max} and P^f_{max} are the maximum transmit powers of the VU transmitters and FUs, respectively, p_v is the maximum outage probability of the V2V links, p_f is the maximum outage probability of the F2FS links, γ^v_{th} and γ^f_{th} are the SINR thresholds for the V2V and F2FS links, respectively, and $b_{m,j}$ is the channel assignment indicator for each FU such that $b_{m,j} = 1$ if the m-th FU transmits over the j-th channel and $b_{m,j} = 0$ otherwise. (8a) ensures that the transmit powers of each VU transmitter for both V2I and V2V links are non-negative and the total transmit power of each VU transmitter is positive and within the maximum VU transmit power. (8b) is the aforementioned power difference condition. (8c) ensures that the transmit power of each FU is non-negative and within the maximum FU transmit power. (8d) and (8e) represent the reliability requirements for V2V and F2FS links, respectively. (8f) reveals the binary properties of both VU and FU channel assignment indicators. (8g) guarantees that each channel can only be assigned by one VU transmitter and each VU transmitter can only occupy one channel. Similarly, (8h) ensures that each channel can only be assigned by one FU and each FU can only occupy one channel. Note that, for each channel, one VU transmitter and one FU can coexist.

Obviously, (8) is a mixed-integer, non-convex, and chance-constrained problem, which cannot be effectively solved via existing methods. Moreover, the optimal solution requires exhaustive search over combinatorial space of binary variables $a_{i,j}$ and $b_{m,j}$, which results in prohibitive computational complexity in practice. To obtain satisfactory results with low complexity, we will decouple (8) into the proposed cascaded channel assignment, through which VUs and FUs are paired, and the power allocation for each VU-FU pair.

III. Cascaded Channel Assignment

To relax the binary and combinatorial constraints in (8), we propose in this section a cascaded channel assignment algorithm based on the Hungarian algorithm with polynomial complexity [29].

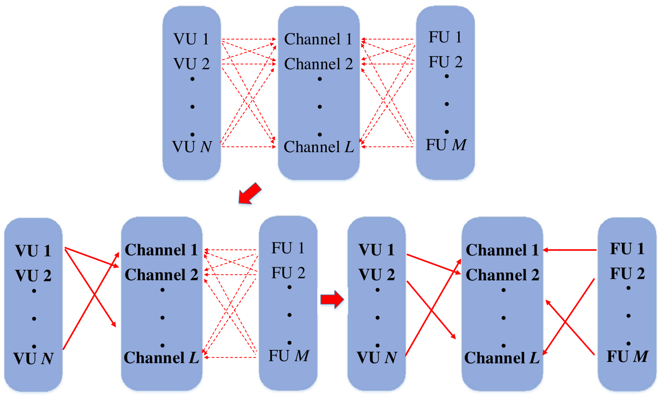

Fig. 2. Cascaded channel assignment.

The channel assignment in (8) involves two goals. The first one is to assign channels to VUs for the throughput maximization of V2I links while guaranteeing the reliability of V2V links. The second goal is to share channels with FUs, limit the introduced interference to VUs, and maintain their own reliability. Instead of exhaustive search, the Hungarian algorithm is an effective combinatorial optimization algorithm for assignment problems [30]. With the Hungarian algorithm, optimality can be achieved by either maximizing the overall throughput of V2I links or minimizing the total introduced interference to VUs. However, since the channel assignments of VUs and FUs affect each other in our scenario, applying the Hungarian algorithm to the channel assignments of VUs and FUs individually cannot guarantee the two goals to be satisfied at the same time. Therefore, a cascaded channel assignment algorithm is proposed to simultaneously meet the two requirements. The logic of the proposed cascaded channel assignment is illustrated in Fig. 2. The original channel assignment between VUs, FUs, and channels is shown as a 3-d combinational assignment problem in Fig. 2, with no effective algorithm to obtain the optimal solution within polynomial time. The intuitive optimal solution, i.e., exhaustive search, requires exponential time. In our proposed cascaded channel assignment, the assignment of channels to VUs is first conducted to reduce the 3-d assignment problem to a 2-d assignment problem, in which the V2X requirements are satisfied. Based on the channel assignment of VUs, the assignment of channels to FUs is then conducted. In our proposed cascaded channel assignment, not only the various QoS requirements can be satisfied but also the computational complexity is reduced.

A. Cascaded Channel Assignment Algorithm

Given that the reliability of V2V links is more important than that of F2FS links from the safety perspective, we assume that VUs have priorities to access channels. Before the channel assignment is determined, the optimal powers cannot be allocated and the throughput of V2I links and interference from FUs to VUs cannot be calculated at this stage. Therefore, the proposed cascaded channel assignment consists of two phases. Firstly, channels are assigned to VUs according to the Hungarian algorithm to maximize the overall throughput of V2I links based on the *channel to noise ratios* (CNRs). With the channel assignment of VUs, the CNR of the interference link from FUs over each channel is determined through the calculation of the CNR of the interference link from FUs to the VU who occupies that channel. Secondly, the Hungarian algorithm is adopted to assign channels to FUs to minimize the total CNR of the interference links from FUs to VUs and thus to minimize the co-channel interference. Let $\phi^v_{i,j}$ denote the V2I link CNR for the i-th VU over the j-th channel and $\phi^f_{m,j}$ the interference link CNR for the m-th FU over the j-th channel. The proposed cascaded channel assignment algorithm is detailed in Algorithm 1.

Algorithm 1 Cascaded Channel Assignment

Initialization: Initialize VU channel assignment matrix $\mathbf{A_{NxL}}$ with entry $a_{i,j} = 0, \forall i, j$, and FU channel assignment channel matrix $\mathbf{B_{MxL}}$ with entry $b_{m,j} = 0, \forall m, j$.
Phase I: VU channel assignment
  for $i = 1 : N$ **do**
    for $j = 1 : L$ **do**
      Calculate $\phi^v_{i,j} = \frac{g^v_{i,j}}{\sigma^2}$.
    end for
  end for
  Use the Hungarian algorithm to find the channel assignment $\mathbf{A}^*$ based on $\{\phi^v_{i,j}\}$.
Phase II: FU channel assignment
  for $m = 1 : M$ **do**
    for $j = 1 : L$ **do**
      if $\sum_{i=1}^N a_{i,j} = 1$
        Find i^* such that $a_{i^*,j} = 1$ according to $\mathbf{A}^*$.
        Calculate $\phi^f_{m,j} = \frac{g^f_{m,i',j}}{\sigma^2}$.
      else
        Set $\phi^f_{m,j} = 0$.
    end for
  end for
  Use the Hungarian algorithm to find the channel assignment $\mathbf{B}^*$ based on $\{\phi^v_{m,i'^*j}\}$.
Return VU and FU channel assignment matrices $\mathbf{A}^*$ and $\mathbf{B}^*$.

Note that the channel assignment is originally a 3-dimensional assignment problem involving VUs, FUs, and channels. The optimal solution can be obtained through exhaustive search, which is treated as the benchmark. In Algorithm 1, the cascaded channel assignment based on the outcome of Phase I reduces to one dimension for FU channel assignment, which simplifies the problem. This is a suboptimal algorithm that requires $\mathcal{O}(NL + ML)$ to calculate link CNRs and $\mathcal{O}(L^3 + L^3)$ for the Hungarian algorithm. In comparison with the optimal exhaustive search whose computational complexity is $\mathcal{O}((\frac{(L!)^2}{(L-M)!(L-N)!})$, the proposed cascaded channel assignment dramatically reduces the computational complexity. Through the proposed cascaded channel assignment, the binary and combinatorial constraints in (8) are relaxed.

B. Hungarian Algorithm Strategies

As stated in Algorithm 1, the ultimate goal of the Hungarian algorithm is to maximize the throughput of V2I links.

Since NOMA is adopted at the VUs, there are three possible strategies for the Hungarian algorithm to assign channels.

- *Based on the V2I link CNRs*: The *Hungarian algorithm based on the V2I link CNRs* (HBV2I) is the most straightforward method to maximize the total CNR of V2I links. The HBV2I scheme directly increases the throughput of V2I links.
- *Based on the V2V link CNRs*: The *Hungarian algorithm based on the V2V link CNRs* (HBV2V) can indirectly improve the throughput of V2I links. Since less transmit power for the V2V links is needed to satisfy the reliability constraints with better V2V link CNRs, more transmit power becomes available for the V2I links under the total transmit power constraint. Therefore, the overall throughput of V2I links can be increased.
- *Based on the difference between the V2I link CNRs and V2V link CNRs*: In power-domain NOMA, the users with more distinctive channel conditions achieve better throughput performance [31]. Therefore, the *Hungarian algorithm based on the difference of V2I link CNRs and V2V link CNRs* (HBD), i.e., $|g^v_{i,i',j} - g^v_{i,j}|$, can be beneficial to the throughput performance of V2I links.

Since our model mainly focuses on the throughput maximization of V2I links while guaranteeing the reliability of V2V links, the HBV2I is adopted in our paper and obtains the best performance improvement due to the direct relationship between the total CNR and the throughput of V2I links although both the HBV2V and HVD can increase the throughput of V2I links. The comparison of the three schemes is provided in the simulation.

IV. Power Allocation

Through the proposed cascaded channel assignment algorithm, the VU and FU who share the same channel form a VU-FU pair. Since different VU-FU pairs adopt orthogonal channels, the power allocation in (8) can be carried out at each single VU-FU pair. However, even with deterministic channel assignments, $a_{i,j}, bm, j$, (8) is still a multi-variable, non-convex, and chance-constrained problem, and it is still difficult to find an optimal solution. To derive an effective power allocation, we first transform the probabilistic constraints into deterministic forms in this section through approximation. Then through the analysis and proposed theorem, we obtain the feasible power allocation region and the optimal solution to the transformed problem.

After the channel assignment is determined, a channel can be shared within an arbitrary VU-FU pair, e.g., the i-th VU shares the j-th channel with the m-th FU. (8) is transformed to

$$\max_{P^v_i, P^v_{i,i'}, P^f_m} \quad \log_2(1+\gamma^v_i) \tag{9}$$

$$\text{s.t.: } 0 \le P^v_i, \quad 0 \le P^v_{i,i'}, \ 0 \le P^v_i + P^v_{i,i'} \le P^v_{max}, \ \forall i, \tag{9a}$$

$$\frac{(P^v_i - P^v_{i,i'})g^v_{i,i',j}}{\sigma^2} \ge \delta, \tag{9b}$$

$$0 \le P^f_m \le P^f_{max}, \tag{9c}$$

$$\Pr(\gamma^v_{i,i'} \ge \gamma^v_{th}) \ge 1 - p_v, \tag{9d}$$

$$\Pr(\gamma^f_m \ge \gamma^f_{th}) \ge 1 - p_f. \tag{9e}$$

Since channel estimation errors exist in the interference links, we substitute (1), (2), and (3) into (9d) and (9e) to evaluate the reliability requirements and have

$$\Pr\Big(\frac{P^v_{i,i'} g^v_{i,i',j}}{P^f_m \alpha^f_{m,i',j} |\hat{h}^f_{m,i',j} + \epsilon|^2 + \sigma^2} \ge \gamma^v_{th}\Big) \ge 1 - p_v \tag{10}$$

and

$$\Pr\Big(\frac{P^f_m g^f_{m,j}}{P^v \alpha^v_{i,m,j} |\hat{h}^v_{i,m,j} + \epsilon|^2 + \sigma^2} \ge \gamma^f_{th}\Big) \ge 1 - p_f, \tag{11}$$

where P^v is the total VU transmit power, i.e., $P^v = P^v_i + P^v_{i,i'}$.

Given the estimated fast fading components $\hat{h}^f_{m,i',j}$ and $\hat{h}^v_{i,m,j}$, $\frac{|\hat{h}^f_{m,i',j}+\epsilon|^2}{\sigma^2_\epsilon}$ and $\frac{|\hat{h}^v_{i,m,j}+\epsilon|^2}{\sigma^2_\epsilon}$ are 2-degree non-central Chi-square distributed with non-centrality parameters $\lambda_f = \frac{2|\hat{h}^f_{m,i',j}|^2}{\sigma^2_\epsilon}$ and $\lambda_v = \frac{2|\hat{h}^v_{i,m,j}|^2}{\sigma^2_\epsilon}$, respectively [32]. Define the corresponding 2-degree non-central Chi-square random variables as $\mathcal{X}^2_{2,nc}$ and $\mathcal{Y}^2_{2,nc}$. Then (10) and (11) can be rearranged as

$$\Pr\Big(\frac{P^v_{i,i'} g^v_{i,i',j} - \sigma^2 \gamma^v_{th}}{\frac{\sigma^2_\epsilon}{2} P^f_m \alpha^f_{m,i',j} \gamma^v_{th}} \ge \mathcal{X}^2_{2,nc}\Big) \ge 1 - p_v \tag{12}$$

and

$$\Pr\Big(\frac{P^f_m g^f_{m,j} - \sigma^2 \gamma^f_{th}}{\frac{\sigma^2_\epsilon}{2} P_v \alpha^v_{i,m,j} \gamma^f_{th}} \ge \mathcal{Y}^2_{2,nc}\Big) \ge 1 - p_f \tag{13}$$

with *probability density functions* (PDFs)

$$f_{\mathcal{X}^2_{2,nc}}(x) = \frac{1}{\sigma^2_\epsilon} \exp\Big(-\frac{|\hat{h}^f_{m,i',j}|^2 + x}{\sigma^2_\epsilon}\Big) I_0\Big(\sqrt{x|\hat{h}^f_{m,i',j}|^2} \frac{2}{\sigma^2_\epsilon}\Big) \tag{14}$$

and

$$f_{\mathcal{Y}^2_{2,nc}}(y) = \frac{1}{\sigma^2_\epsilon} \exp\Big(-\frac{|\hat{h}^v_{i,m,j}|^2 + y}{\sigma^2_\epsilon}\Big) I_0\Big(\sqrt{y|\hat{h}^v_{i,m,j}|^2} \frac{2}{\sigma^2_\epsilon}\Big), \tag{15}$$

where I_0 is the zero-order modified Bessel function of the first kind.

Even with (14) and (15), it is still difficult to obtain closed-form expressions of reliability requirements (12) and (13). Therefore, we adopt an approximation of non-central Chi-square distribution to simplify (12) and (13) [33]. With $\sigma^2_\epsilon = 1$, the approximation is illustrated in Fig. 3.

With some manipulation of the rest constraints, the feasible power region of (8) is given in Lemma 1 and depicted in Fig. 4.

Lemma 1: The feasible power allocation region of (8) is derived in two cases as

Case I: $\frac{B_2}{A_2} > \frac{B_1}{A_1}$ and $\frac{B_2}{A_2}\bar{P}^f_{max} + \frac{C_2}{A_2} \le P^v_{max}$

$$\begin{aligned} \{(P^v_i, P^v_{i,i'}, P^f_m) :& \\ & 0 \le P^f_m \le \bar{P}^f_{max}, P^v_{i,i'} \ge \frac{B_1}{A_1} P^f_m + \frac{C_1}{A_1}, \\ & P^v_i + P^v_{i,i'} \le \frac{B_2}{A_2} P^f_m + \frac{C_2}{A_2}, P^v_{i,i'} \le \frac{P^v_{max} - \frac{\delta\sigma^2}{g^v_{i,i',j}}}{2} \}; \end{aligned} \tag{16}$$

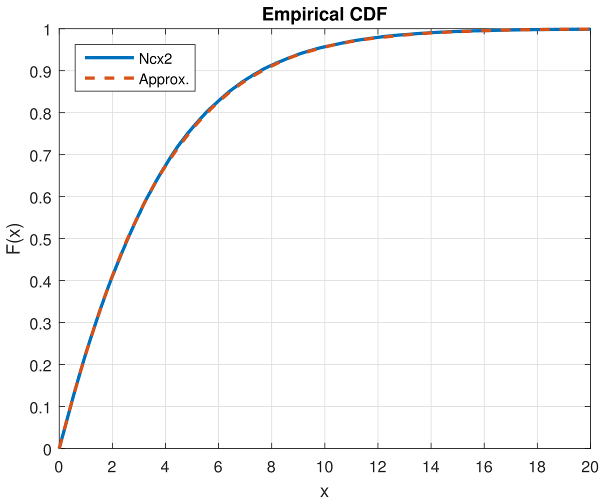

Fig. 3. CDFs of non-central Chi-square distribution (Ncx2) and its approximation (Approx.) with $\sigma_\epsilon^2 = 1$.

Case II: $\frac{B_2}{A_2} > \frac{B1}{A_1}$ and $\frac{B_2}{A_2}\bar{P}^f_{max} + \frac{C_2}{A_2} > P^v_{max}$

$$\begin{aligned}&\{(P^v_i, P^v_{i,i'}, P^f_m):\\ &\quad 0 \le P^f_m \le \bar{P}^f_{max}, P^v_{i,i'} \ge \frac{B_1}{A_1}P^f_m + \frac{C_1}{A_1},\\ &\quad P^v_i + P^v_{i,i'} \le \frac{B_2}{A_2}P^f_m + \frac{C_2}{A_2}, P^v_{i,i'} \le \frac{P^v_{max} - \frac{\delta\sigma^2}{g^v_{i,i',j}}}{2},\\ &\quad P^v_i + P^v_{i,i'} \le P^v_{max}\}, \end{aligned} \tag{17}$$

where $A_1 = \frac{g^v_{i,i',j}}{\gamma^v_{th}}$, $B_1 = \frac{\sigma_\epsilon^2}{2}(1+\frac{\lambda_f}{2})\alpha^f_{m,i',j}\ln\frac{1}{p_v^2}$, $C_1 = \sigma^2$, $A_2 = \frac{\sigma_\epsilon^2}{2}(1+\frac{\lambda_v}{2})\alpha^v_{i,m,j}\ln\frac{1}{p_f^2}$, $B_2 = \frac{g^f_{m,j}}{\gamma^f_{th}}$, $C_2 = -\sigma^2$, and $\bar{P}^f_{max} = \min\{\frac{A_1(P^v_{max} - \frac{\delta\sigma^2}{g^v_{i,i',j}}) - 2C_1}{2B_1}, P^f_{max}\}$.

Proof: See Appendix A. ∎

Based on Lemma 1, the optimal power allocation solution to (9) is provided in Theorem 1.

Theorem 1: The optimal power allocation solution to (9) is

$$P^{f*}_m = \begin{cases} \bar{P}^f_{max}, & \text{Case I},\\ \frac{A_2}{B_2}P^v_{max} - \frac{C_2}{B_2}, & \text{Case II}, \end{cases} \tag{18}$$

$$P^{v*}_i = \begin{cases} \left(\frac{B_2}{A_2} - \frac{B_1}{A_1}\right)\bar{P}^f_{max} + \left(\frac{C_2}{A_2} - \frac{C_1}{A_1}\right), & \text{Case I},\\ P^v_{max} - \frac{B_1}{A_1}\left(\frac{A_2}{B_2}P^v_{max} - \frac{C_2}{B_2}\right) - \frac{C_1}{A_1}, & \text{Case II}, \end{cases} \tag{19}$$

and

$$P^{v*}_{i,i'} = \begin{cases} \frac{B_1}{A_1}\bar{P}^f_{max} + \frac{C_1}{A_1}, & \text{Case I},\\ \frac{B_1}{A_1}\left(\frac{A_2}{B_2}P^v_{max} - \frac{C_2}{B_2}\right) + \frac{C_1}{A_1}, & \text{Case II}. \end{cases} \tag{20}$$

Proof: See Appendix B. ∎

Theorem 1 gives the optimal power allocation to the transformed throughput optimization problem of V2I links while guaranteeing the reliability of V2V and F2FS links for each VU-FU pair.

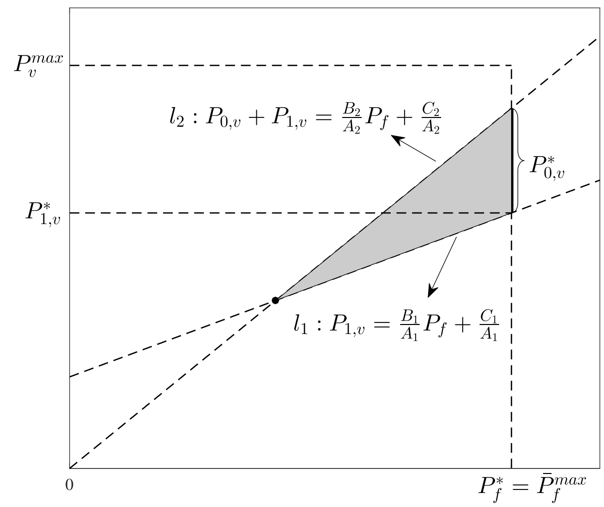

(a) Case I.

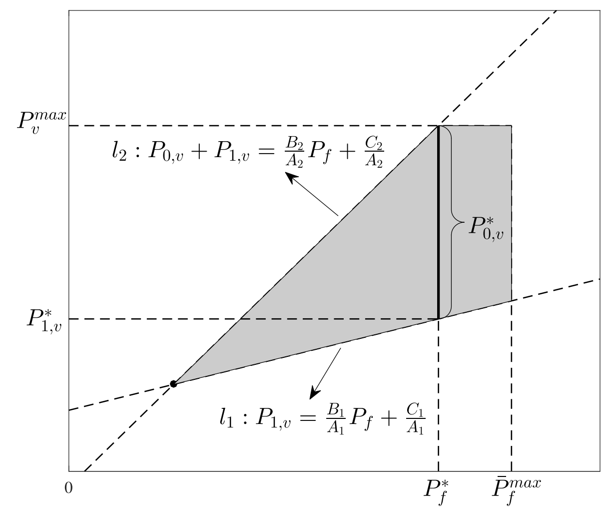

(b) Case II.

Fig. 4. Feasible power allocation region of (9) in two cases.

Since the optimal power allocation has a computational complexity of $\mathcal{O}(\max\{N, M\})$, the computational complexity of the proposed resource allocation scheme based on Hungarian algorithm is $\mathcal{O}((M+N)L + L^3 + \max\{N, M\})$. In comparison, the computational complexity of the optimal search and power allocation is $\mathcal{O}((\frac{(L!)^2}{(L-M)!(L-N)!})\cdot\max\{N, M\})$. Therefore, the proposed resource allocation scheme significantly reduces the computational complexity.

V. Simulation Results

In this section, we present simulation results to illustrate the performance of the proposed resource allocation scheme in a heterogeneous vehicular network. We simulate a two-way urban roadway scenario. The vehicles are covered by a single macrocell and several non-overlapping coexisting femtocells as illustrated in Fig. 1. The VUs are dropped according to a spatial Poisson point process with density determined by the vehicle speed. The FUs are generated by a spatial Poisson point process with density 8 per femtocell. Each VU sets up a V2V link to the nearest VU behind and the coexisting FU is randomly selected from the generated FUs. The numbers of

TABLE I
SIMULATION PARAMETERS

Parameter	Value
Carrier frequency	2 GHz
Macrocell radius	500 m
Femtocell radius	50 m
Vehicle speed s	60 km/h
Vehicle density	$2.5s$, s in m/s
FU density	8/2500 /m^2
SINR threshold for V2V link γ_v^{th}	5 dB
SINR threshold for F2FS link γ_f^{th}	5 dB
Reliability for V2V link p_v	10^{-3}
Reliability for F2FS link p_f	10^{-3}
Maximum VU transmit power P_v^{max}	23 dBm
Maximum FU transmit power P_f^{max}	10 dBm
Noise power σ^2	-114 dBm
Required power difference ratio δ	10 dB

selected VUs and FUs, N and M, are both 4. The total number of channels, L, is 4. The major simulation parameters are listed in Table I [9], [10], [19]. In our simulation, the V2I, V2FS, and F2FS links are modeled as *non-line-of-sight* (NLOS) while the V2V and F2V links are modeled as *line-of-sight* (LOS). The NLOS and LOS pathloss models are $128.1 + 37.6 \log_{10} d$ and WINNER + B1 [34], respectively.

In Fig. 5, the overall throughput of the V2I links with different schemes and channel estimation errors is shown. In Fig. 5(a), the proposed NOMA resource allocation scheme is compared with the OMA resource allocation scheme and NOMA power allocation with exhaustive search under different channel estimation errors. Since the V2I link throughput with NOMA is indirectly affected by the outage probabilities, the increase of V2I link throughput is limited. Although the exhaustive search renders the best performance, the complexity is prohibited in practice. Our proposed NOMA resource allocation scheme achieves comparable performance with the exhaustive search and outperforms the OMA resource allocation. However, due to the interference from the V2V links to the V2I links, the proposed NOMA resource allocation scheme results in less than double throughput performance of the OMA resource allocation. It can be noticed that larger channel estimation errors degrade the performance with NOMA power allocation, but has little influence on that of OMA power allocation when different links use orthogonal channels. In Fig. 5(b), the performance of different Hungarian channel assignment schemes are illustrated. Without consideration of computational complexity, the exhaustive search provides the best performance. It is obvious that HBV2I achieves better performance than HBV2V and HBD due to the direct relationship between the V2I link CNRs and throughput. Since HBV2V only considers the V2V link CNRs, the overall throughput of the V2I links with HBV2V is the lowest.

In Fig. 6, the comparison of the overall throughput of V2I links in the proposed method and Fang's method [20] is shown. Note that Fang's method focuses on energy efficiency while ours focuses on the throughput, where we apply the user scheduling algorithm to assign channels and the iterative power allocation methodology. It is clear that our proposed method achieves higher throughput in comparison with Fang's method. This is because that Fang's method

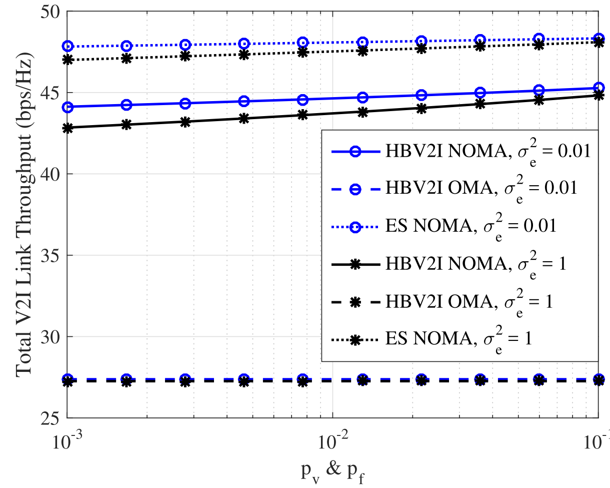

(a) NOMA vs OMA with different channel estimation errors.

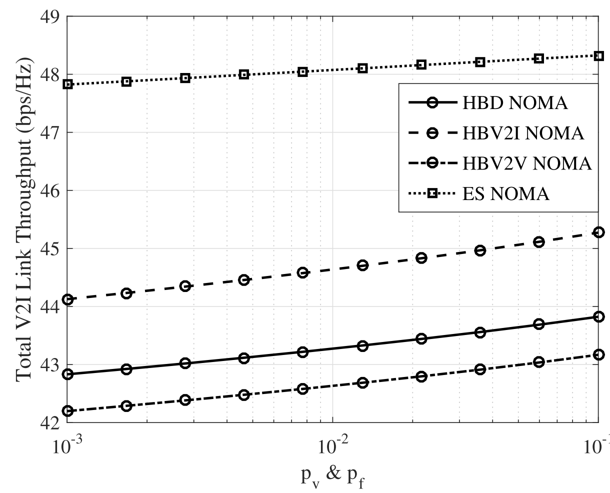

(b) HBV2I vs HBV2V vs HBD with $\sigma_e^2 = 0.01$.

Fig. 5. Overall throughput of V2I links with different channel estimation errors and schemes.

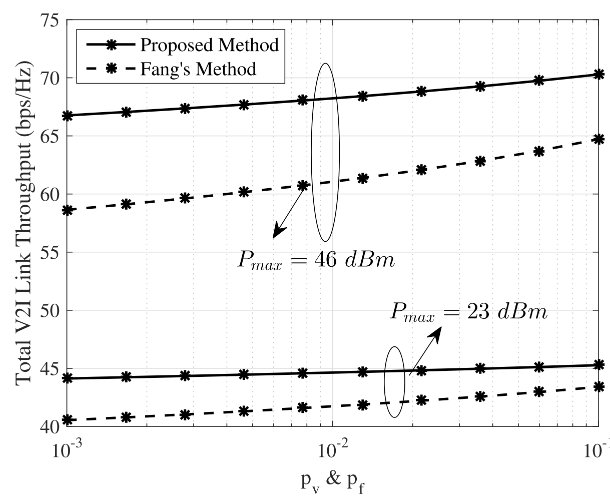

Fig. 6. Comparison of overall throughput of V2I links in the proposed method and Fang's method with $p_v = p_f = 10^{-3}$ and $\gamma_v^{th} = \gamma_f^{th} = 5$ dB.

preserves the transmit power for better energy efficiency, while our proposed method fully utilizes the transmit power to maximize the throughput. With larger maximum transmit powers,

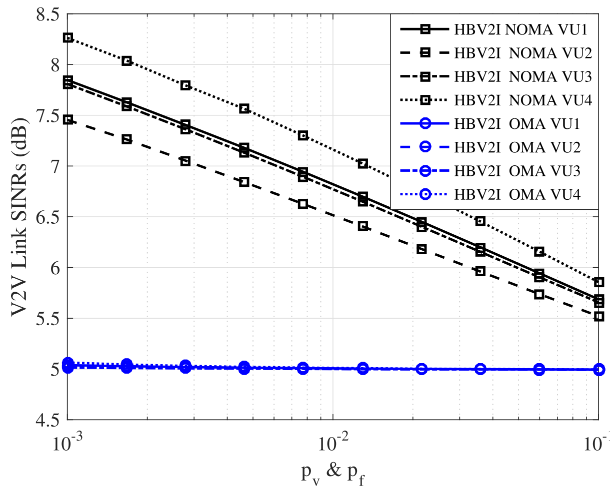

(a) NOMA vs OMA with $\sigma_e^2 = 0.01$ for 4 VUs.

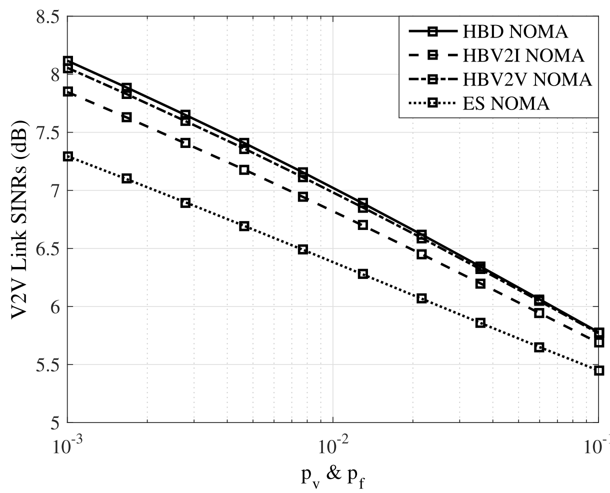

(b) HBV2I vs HBV2V vs HBD with $\sigma_e^2 = 0.01$ for VU1.

Fig. 7. SINRs of V2V links with different schemes and $\sigma_e^2 = 0.01$.

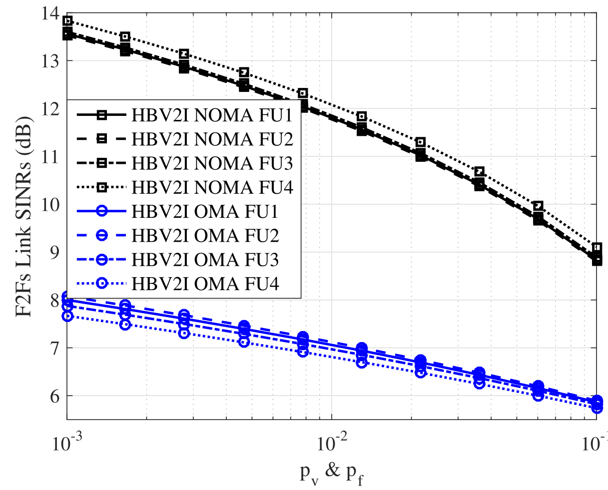

(a) NOMA vs OMA with $\sigma_e^2 = 0.01$ for 4 FUs.

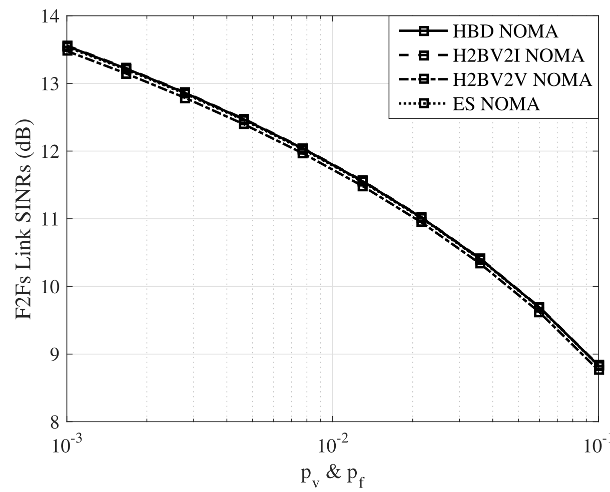

(b) HBV2I vs HBV2V vs HBD with $\sigma_e^2 = 0.01$ for FU1.

Fig. 8. The SINRs of F2FS links with different schemes and $\sigma_e^2 = 0.01$.

our proposed method exhibits more benefits, as higher powers can be allocated to improve the throughput.

In Fig. 7, the SINRs of the V2V links with different schemes and $\sigma_e^2 = 0.01$ are illustrated. Fig. 7(a) shows the SINRs of the V2V links for all 4 VUs in NOMA and OMA. It is obvious that both NOMA and OMA can satisfy the minimum SINR requirement, i.e., 5 dB. Since the channel estimation error in NOMA from the V2I link to the V2V link is considered in (8d), there are some margins for SINRs in NOMA to guarantee the outage probability constraint. In contrast, no interference exists in OMA and thus no protection margins are needed. Therefore, the power allocation in OMA assigns the V2V transmit power to maintain the minimum SINR requirement. In Fig. 7(b), VU1's V2V link SINRs with different channel allocation schemes are illustrated. The exhaustive search for channel allocation has the minimum SINR margin to guarantee the outage probability constraint. The HBV2I outperforms the HBV2V and HBD schemes with less V2V link SINR margin, which can allocate more transmit power to V2I links while satisfying the reliability requirements.

In Fig. 8, the SINRs of the F2FS links with different schemes and $\sigma_e^2 = 0.01$ are shown. The required SINR for F2FS links is also 5 dB. As shown in Fig. 8(a), the SINRs of the F2FS links with our proposed NOMA scheme still have larger SINR margins than those with OMA scheme to guarantee the reliability constraint in our formulated problem, which is the same for the V2V links. However, the SINRs of the F2FS links with OMA scheme also have SINR margins due to the fact that in OMA scheme, FUs still coexist with VUs and have to consider the interference and channel estimation errors. In Fig. 8(b), different channel assignment schemes render similar SINRs of F2FS links. This is because in NOMA, the F2FS links share the channel with both the V2I and V2V links, no matter how different VU transmit powers are allocated to V2I and V2V links. The interference from the VU to FU depends on the total VU transmit power, which equals the maximum VU transmit power in order to maximize the throughput of V2I links as long as the outage probability constraint of F2FS links can be satisfied.

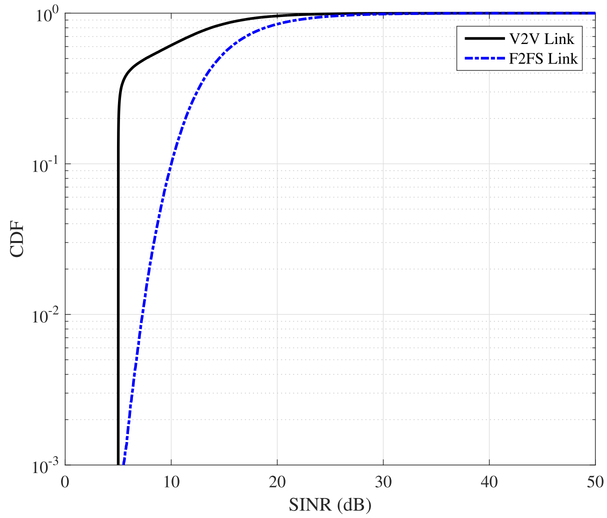

Fig. 9. CDFs of V2V and F2FS links versus SINR with $p_v = p_f = 10^{-3}$ and $\gamma_v^{th} = \gamma_f^{th} = 5$ dB for VU1 and its co-existing FU.

Fig. 9 shows the *cumulative distribution functions* (CDFs) of the V2V and F2FS links with respect to the SINR for VU1 and its co-existing FU. It can be seen that the V2V link achieves the reliability requirement with our proposed resource allocation scheme. However, since P_i^v exists in (7), the approximation error of non-central Chi-square distribution is amplified in the F2FS link, which renders the SINR of F2FS link slightly larger than the desired threshold, i.e., 5 dB, at the target outage probability. Moreover, due to P_m^f in the numerator of γ_m^f and P_i^v in the denominator, a larger P_m^f allows a larger P_i^v, which increases the throughput of V2I link. Meanwhile, a larger P_m^f may result in a larger SINR of F2FS link, which is reflected in Fig. 9 with a larger probability of higher SINR of F2FS link than that of V2V link. Because the V2V link competes for resource with the V2I link, a large percentage of V2V link SINRs stick around the desired threshold, i.e., 5 dB, to maximize the transmit power for the V2I link.

VI. Conclusions

In this paper, we investigate the robust resource allocation problem for heterogeneous vehicular communications with imperfect channel estimation. NOMA is adopted in the network to increase spectral efficiency. Considering the imperfect channel estimation, we formulate a chance-constrained optimization problem to maximize the throughput of V2I links and retain the reliability requirements of V2V and F2FS links at the same time. To simplify and decouple the joint power and channel assignment problem, we derive a cascaded Hungarian channel assignment algorithm. With the assigned channels, we transform the chance constraints into deterministic ones through the approximation of non-central Chi-square distribution and derive the corresponding feasible region and optimal power allocation. In our simulation, we illustrate the effectiveness and superiority of the proposed resource allocation scheme. In our future work, we will study advanced dynamic user scheduling and pairing schemes to further enhance the performance of heterogeneous vehicular communications.

Appendix A
Proof of Lemma 1

Proof: Rearranging (9a) and (9b), we obtain

$$P_{i,i'}^v \leq \frac{P_{max}^v - \frac{\delta\sigma^2}{g_{i,i',j}^v}}{2}, \tag{21}$$

which limits $P_{i,i'}^v$ to guarantee successful SIC at the VU receiver. According to [33], the CDF of 2-degree Chi-square distribution, $\mathcal{X}_2^2$, can be used to approximate the CDF of 2-degree non-central Chi-square distribution with non-centrality parameter λ, that is

$$\begin{aligned} &Pr(\mathcal{X}_{2,nc}^2 \leq x) \\ &\quad \approx Pr(\mathcal{X}_2^2 \leq \frac{x}{1+\lambda^2/2}) \\ &\quad = 1 - e^{(-\frac{\frac{x}{1+\lambda^2/2}}{2})}. \end{aligned} \tag{22}$$

With the substitution of (22) into (12) and (13) and some mathematical manipulations, the power allocation should satisfy

$$P_{i,i'}^v \geq \frac{B_1}{A_1} P_m^f + \frac{C_1}{A_1} \tag{23}$$

and

$$P_i^v + P_{i,i'}^v \leq \frac{B_2}{A_2} P_m^f + \frac{C_2}{A_2}. \tag{24}$$

Because $C_1 > 0$, $C_2 < 0$, and $P_i^v + P_{i,i'}^v \geq P_{i,i'}^v$, $\frac{B_2}{A_2} > \frac{B_1}{A_1}$ is necessary to ensure a feasible region. With $\frac{B_1}{A_1} > 0$, (21), and (23), P_m^f cannot go beyond $\frac{A_1(P_{max}^v - \frac{\delta\sigma^2}{g_{i,i',j}^v}) - 2C1}{2B1}$. Define $\bar{P}_{max}^f$ as $\min\{\frac{A_1(P_{max}^v - \frac{\delta\sigma^2}{g_{i,i',j}^v}) - 2C1}{2B1}, P_{max}^f\}$, we have $P_m^f \leq \bar{P}_{max}^f$. According to (24), $P_i^v + P_{i,i'}^v \leq \frac{B_2}{A_2}\bar{P}_{max}^f + \frac{C_2}{A_2}$ needs to be satisfied.

In consideration of (8a), if $\frac{B_2}{A_2}\bar{P}_{max}^f + \frac{C_2}{A_2} \leq P_{max}^v$, we have the feasible power region in Case I; if $\frac{B_2}{A_2}\bar{P}_{max}^f + \frac{C_2}{A_2} > P_{max}^v$, $P_i^v + P_{i,i'}^v \leq P_{max}^v$ should be considered and we have the feasible power region in Case II, which completes the proof. ∎

Appendix B
Proof of Theorem 1

Proof: Observing (9), we clearly note that the objective function of (9) monotonically increases with increasing P_i^v and decreases with increasing $P_{i,i;}^v$. Therefore, given P_m^f and (23), $P_{i,i'}^v$ should reside on the lower boundary for a smaller $P_{i,i'}^v$. Similarly, $P_i^v + P_{i,i'}^v$ must reside on the upper boundary for a larger P_i^v given $P_{i,i'}^v$.

Therefore, we have in Case I

$$P_{i,i'}^v = \frac{B_1}{A_1} P_m^f + \frac{C_1}{A_1} \tag{25}$$

and

$$P_i^v + P_{i,i'}^v = \frac{B_2}{A_2} P_m^f + \frac{C_2}{A_2}. \tag{26}$$

The objective function of (9) can be expressed as

$$R_i^v = \log_2(1 + \frac{[(\frac{B_2}{A_2} - \frac{B_1}{A_1})P_m^f + \frac{C_2}{A_2} - \frac{C_1}{A_1}]g_{i,j}^v}{(\frac{B1}{A1}P_m^f + \frac{C_1}{A_1})g_{i,j}^v + \sigma^2}). \tag{27}$$

Because the derivative of R_i^v with respect to P_m^f is greater than 0 in the feasible region, R_i^v increases with increasing P_m^f in the feasible region. Therefore, the optimal P_m^f for Case I is $P_m^{f*} = \bar{P}_{max}^f$. Substituting P_m^{f*} into (25) and (26), we can obtain $P_{i,i'}^{v*}$ and P_i^{v*} for Case I as

$$P_{i,i'}^{v*} = \frac{B_1}{A_1}\bar{P}_f^{max} + \frac{C_1}{A_1} \tag{28}$$

and

$$P_i^{v*} = (\frac{B_2}{A_2} - \frac{B_1}{A_1})\bar{P}_{max}^f + (\frac{C_2}{A_2} - \frac{C_1}{A_1}), \tag{29}$$

respectively.

In Case II, when $\frac{B_2}{A_2}P_m^f + \frac{C_2}{A_2} < P_{max}^v$, the objective function of (9) is the same as (27) and increases with increasing P_m^f. When $\frac{B_2}{A_2}P_m^f + \frac{C_2}{A_2} \geq P_{max}^v$, the objective function of (9) can be rewritten as

$$R_i^{'v} = \log_2{(1 + \frac{(P_{max}^v - \frac{B_1}{A_1}P_m^f - \frac{C_1}{A_1})g_{i,j}^v}{(\frac{B1}{A1}P_m^f + \frac{C_1}{A_1})g_{i,j}^v + \sigma^2})}, \tag{30}$$

which decreases with increasing P_m^f. Therefore, the maximum of (9) is reached when $\frac{B_2}{A_2}P_m^{f*} + \frac{C_2}{A_2} = P_{max}^v$ is satisfied for Case II. Specifically, $P_m^{f*} = \frac{A_2}{B_2}P_{max}^v - \frac{C_2}{B_2}$. Similar to Case I, $P_{i,i'}^{v*}$ and P_i^{v*} for Case II are

$$P_{i,i'}^{v*} = \frac{B_1}{A_1}(\frac{A_2}{B_2}P_{max}^v - \frac{C_2}{B_2}) + \frac{C_1}{A_1} \tag{31}$$

and

$$P_i^{v*} = P_{max}^v - \frac{B_1}{A_1}(\frac{A_2}{B_2}P_{max}^v - \frac{C_2}{B_2}) - \frac{C_1}{A_1}, \tag{32}$$

respectively.

Combining the two cases, we complete the proof. ■

References

[1] S. Guo and X. Zhou, "Robust power allocation for NOMA in heterogeneous vehicular communications with imperfect channel estimation," in *Proc. IEEE Int. Symp. Pers., Indoor, Mobile Radio Commun.*, Montreal, QC, Canada, Oct. 2017, pp. 1–5.

[2] G. Araniti, C. Campolo, M. Condoluci, A. Iera, and A. Molinaro, "LTE for vehicular networking: A survey," *IEEE Commun. Mag.*, vol. 51, no. 5, pp. 148–157, May 2013.

[3] K. Zheng, Q. Zheng, P. Chatzimisios, W. Xiang, and Y. Zhou, "Heterogeneous vehicular networking: A survey on architecture, challenges, and solutions," *IEEE Commun. Surveys Tuts.*, vol. 17, no. 4, pp. 2377–2396, 4th Quart., 2015.

[4] *Scenarios, Requirements and KPIs for 5G Mobile and Wireless System*, document ICT-317669-METIS/D1.1, METIS, METIS deliverable D1.1, Apr. 2013. [Online]. Available: https://www.metis2020.com/documents/deliverables/

[5] *IEEE Standard for Information Technology–Telecommunications and Information Exchange Between Systems Local and Metropolitan Area Networks–Specific Requirements—Part 11: Wireless LAN Medium Access Control (MAC) and Physical Layer (PHY) Specifications*, Standard 802.11-2012, Dec. 2016.

[6] A. Bazzi, B. M. Masini, A. Zanella, and I. Thibault, "On the performance of IEEE 802.11p and LTE-V2V for the cooperative awareness of connected vehicles," *IEEE Trans. Veh. Technol.*, vol. 66, no. 11, pp. 10419–10432, Nov. 2017.

[7] S. Chen, J. Hu, Y. Shi, and L. Zhao, "LTE-V: A TD-LTE-based V2X solution for future vehicular network," *IEEE Internet Things J.*, vol. 3, no. 6, pp. 997–1005, Dec. 2016,

[8] R. Molina-Masegosa and J. Gozalvez, "LTE-V for sidelink 5G V2X vehicular communications: A new 5G technology for short-range vehicle-to-everything communications," *IEEE Veh. Technol. Mag.*, vol. 12, no. 4, pp. 30–39, Dec. 2017.

[9] L. Liang, G. Y. Li, and W. Xu, "Resource allocation for D2D-enabled vehicular communications," *IEEE Trans. Commun.*, vol. 65, no. 7, pp. 3186–3197, Jul. 2017.

[10] *3rd Generation Partnership Project; Technical Specification Group Radio Access Network; Study on LTE-based V2X Services*, document 3GPP TR 36.885 V2.0.0 (Release 14), Jun. 2016.

[11] H. Zhang, X. Tang, R. Banez, P. Ren, L. Song, and Z. Han, "An EPEC analysis for power allocation in LTE-V networks," in *Proc. IEEE Global Commun. Conf.*, Singapore, Dec. 2017, pp. 1–6.

[12] Q. Wei, W. Sun, B. Bai, Li Wang, E. G. Ström, and M. Song, "Resource allocation for V2X communications: A local search based 3D matching approach," in *Proc. IEEE Int. Conf. Commun.*, Paris, France, May 2017, pp. 1–6.

[13] J. Mei, K. Zheng, L. Zhao, Y. Teng, and X. Wang, "A latency and reliability guaranteed resource allocation scheme for LTE V2V communication systems," *IEEE Trans. Wireless Commun.*, vol. 17, no. 6, pp. 3850–3860, Jun. 2018.

[14] B. Di, L. Song, Y. Li, and Z. Han, "V2X meets NOMA: Non-orthogonal multiple access for 5G-enabled vehicular networks," *IEEE Wireless Commun.*, vol. 24, no. 6, pp. 14–21, Dec. 2017.

[15] B. Di, L. Song, Y. Li, and G. Y. Li, "Non-orthogonal multiple access for high-reliable and low-latency V2X communications in 5G systems," *IEEE J. Sel. Areas Commun.*, vol. 35, no. 10, pp. 2383–2397, Oct. 2017.

[16] H. Zhang, Y. Ma, D. Yuan, and H.-H. Chen, "Quality-of-service driven power and sub-carrier allocation policy for vehicular communication networks," *IEEE J. Sel. Areas Commun.*, vol. 29, no. 1, pp. 197–206, Jan. 2011.

[17] Y. Han, E. Ekici, H. Kremo, and O. Altintas, "Resource allocation algorithms supporting coexistence of cognitive vehicular and IEEE 802.22 networks," *IEEE Trans. Wireless Commun.*, vol. 16, no. 2, pp. 1066–1079, Feb. 2017.

[18] W. Sun, D. Yuan, E. Ström, and F. Brännström, "Cluster-based radio resource management for D2D-supported safety-critical V2X communications," *IEEE Trans. Wireless Commun.*, vol. 15, no. 4, pp. 2756–2769, Apr. 2016.

[19] L. Liang, J. Kim, S. C. Jha, K. Sivanesan, and G. Y. Li, "Spectrum and power allocation for vehicular communications with delayed CSI feedback," *IEEE Wireless Commun. Lett.*, vol. 6, no. 4, pp. 458–461, Aug. 2017.

[20] F. Fang, H. Zhang, J. Cheng, S. Roy, and V. C. M. Leung, "Joint user scheduling and power allocation optimization for energy-efficient NOMA systems with imperfect CSI," *IEEE J. Sel. Areas Commun.*, vol. 35, no. 12, pp. 2874–2885, Dec. 2017.

[21] H. Zhang, F. Fang, J. Cheng, K. Long, W. Wang, and V. C. M. Leung, "Energy-efficient resource allocation in NOMA heterogeneous networks," *IEEE Wireless Commun.*, vol. 25, no. 2, pp. 48–53, Apr. 2018.

[22] Z. Wei, D. W. K. Ng, J. Yuan, and H.-M. Wang, "Optimal resource allocation for power-efficient MC-NOMA with imperfect channel state information," *IEEE Trans. Commun.*, vol. 65, no. 9, pp. 3944–3961, Sep. 2017.

[23] L. P. Qian, Y. Wu, H. Zhou, and X. Shen, "Non-orthogonal multiple access vehicular small cell networks: Architecture and solution," *IEEE Netw.*, vol. 31, no. 4, pp. 15–21, Jul./Aug. 2017.

[24] Y. Chen, L. Wang, Y. Ai, B. Jiao, and L. Hanzo, "Performance analysis of NOMA-SM in vehicle-to-vehicle massive MIMO channels," *IEEE J. Sel. Areas Commun.*, vol. 35, no. 12, pp. 2653–2666, Dec. 2017.

[25] Z. Ding, P. Fan, and H. V. Poor, "User pairing in non-orthogonal multiple access downlink transmissions," in *Proc. IEEE Global Commun. Conf.*, San Diego, CA, USA, Dec. 2015, pp. 1–5.

[26] Y. Sun, D. W. K. Ng, Z. Ding, and R. Schober, "Optimal joint power and subcarrier allocation for full-duplex multicarrier non-orthogonal multiple access systems," *IEEE Trans. Commun.*, vol. 65, no. 3, pp. 1077–1091, Mar. 2017.

[27] Z. Yang, Z. Ding, P. Fan, and G. K. Karagiannidis, "On the performance of non-orthogonal multiple access systems with partial channel information," *IEEE Trans. Commun.*, vol. 64, no. 2, pp. 654–667, Feb. 2016.

[28] S. Ali, E. Hossain, and D. I. Kim, "Non-orthogonal multiple access (NOMA) for downlink multiuser MIMO systems: User clustering, beamforming, and power allocation," *IEEE Access*, vol. 5, pp. 565–577, 2016.

[29] D. B. West, *Introduction to Graph Theory*, 2nd ed. Cambridge, U.K.: Cambridge Univ. Press, 2001.

[30] H. W. Kuhn, "The Hungarian method for the assignment problem," *Naval Res. Logistics Quart.*, vol. 2, nos. 1–2, pp. 83–97, Mar. 1955.

[31] Z. Ding, P. Fan, and H. V. Poor, "Impact of user pairing on 5G nonorthogonal multiple-access downlink transmissions," *IEEE Trans. Veh. Technol.*, vol. 65, no. 8, pp. 6010–6023, Aug. 2016.

[32] N. Y. Soltani, S. J. Kim, and G. B. Giannakis, "Chance-constrained optimization of OFDMA cognitive radio uplinks," *IEEE Trans. Wireless Commun.*, vol. 12, no. 3, pp. 1098–1107, Mar. 2013.

[33] D. R. Cox and N. Reid, "Approximations to noncentral distributions," *Can. J. Statist.*, vol. 15, no. 2, pp. 105–114, Jun. 1987.

[34] *WINNER II Channel Models*, document IST-4-207756 WINNER II D1.1.2V1.2, Sep. 2007. [Online]. Available: http://projects.celticinitiativeorg/winner+/WINNER2-Deliverables/D1.1.2v1.1.pdf

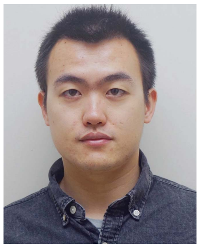

Shengjie Guo received the B.Eng. degree from the University of Electronic Science and Technology of China, Chengdu, China, in 2012. He is currently pursuing the Ph.D. degree with Louisiana State University, Baton Rouge, LA, USA. His research interests include spectrum- and energy-efficient communications, simultaneous wireless information & power transfer, device-to-device communications, and vehicular communications.

Xiangwei Zhou received the B.S. degree in communication engineering from the Nanjing University of Science and Technology, Nanjing, China, in 2005, the M.S. degree in information and communication engineering from Zhejiang University, Hangzhou, China, in 2007, and the Ph.D. degree in electrical and computer engineering from the Georgia Institute of Technology, Atlanta, GA, USA, in 2011. Since 2015, he has been an Assistant Professor with the Division of Electrical and Computer Engineering, Louisiana State University, Baton Rouge, LA, USA. Prior to that, he was an Assistant Professor with the Department of Electrical and Computer Engineering, Southern Illinois University, Carbondale, IL, USA, from 2013 to 2015, and a Senior Systems Engineer with Marvell Semiconductor, Santa Clara, CA, USA, from 2011 to 2013. His research interests include wireless communications, statistical signal processing, and cross-layer optimization, with current emphasis on spectrum-efficient, energy-efficient and secure communications, coexistence of wireless systems, and machine learning for intelligent communications. He was a recipient of the Best Paper Award at the 2014 International Conference on Wireless Communications and Signal Processing.